Journal of Bioscience and Biotechnology Discovery
Volume 8(3), pages 81-91, June 2023
Article Number: B5A675872
ISSN: 2536-7064
https://doi.org/10.31248/JBBD2023.184
https://integrityresjournals.org/journal/JBBD

Full Length Research

Modulation of mitochondrial membrane permeability transition pore by *Annonaceous acetogenins* (ACGs)-Loaded Transferrin Conjugated Nanoparticles

Avan Erhunmwunsee Dalton[1]*, Ngozi Paulinus Okolie[1], Ojowu Johhn Ojowu[2] and Faluyi Ezekiel[3]

[1]Department of Biochemistry, University of Benin, Edo State, Nigeria.
[2]Department of Biochemistry, Federal University of Agriculture, Markudi, Benue State, Nigeria.
[3]Department of Chemistry, University of Ibadan, Oyo State, Nigeria.

*Corresponding author. Email: avandalton68@gmail.com

Received 27th April 2023; Accepted 7th June 2023

ABSTRACT: Making the optimal cancer treatment choice can be challenging and more challenging is harnessing the therapeutic potential of bioactive molecules isolated from plants. The mitochondrion is the main organelle of oxidative stress in cells. Increased permeability of the inner mitochondrial membrane is a key phenomenon in cell death. The protein transferrin (Tf) was conjugated to the NPs with the role to actively targeting them to the cancerous cells. Peg-GNPs, Tf-GNPs, Peg-G-ACGs and Tf-Peg-G-ACGs were successfully synthesized by probe sonication method and yielded NPs with size about 100 nm, with polydispersity index around 0.20 and a negative zeta potential of about − 30 mV. Mitochondria, isolated from rat liver were exposed to different concentrations of Tf-peg-G-ACGs. Their ability to induce mitochondrial permeability transition (mPT) pore opening were assessed spectrophotometrically. In the absence of $CaCl_2$, Tf-peg-G-ACGs caused a concentration-dependent induction of mPT pore opening by 13, 11.3, 8.7, and 2.7 folds, at concentrations 10, 20,50 and 100 µg/mL, respectively, when compared with the control with no attendant inhibitory activity which was intensified in the presence of Calcium to 22, 19.7, 15 and 8.3 folds at concentrations 10, 20,50 and 100 µg/mL, respectively. Tf-peg-G-ACGs showed improved ability to induced mitochondrial membrane pore opening which can be explored for the treatment of cancer.

Keywords: *Annonaceous acetogenins*, mitochondrial targeting, nanomedicine, transferrin.

INTRODUCTION

Targeted nanoparticles have been the subject of intense research for over a decade in order to deliver numerous anticancer medications to the desired tumor site. An advantageous quality for the delivery of anticancer medications is that nanoparticles show an increased permeability and retention (EPR) impact in tumor tissues (Dutta *et al*., 2021; Gavas *et al*., 2021; Fang *et al*., 2023). Active-targeted nano-carriers significantly reduce off-target effects, as is becoming increasingly clear, mostly as a result of their directed localization in tumors and active cellular uptake. Protein-linked nanosystems have been developed in this context to take advantage of the overexpression of receptors on the surface of tumor cells, with the expectation that the biomarker grafting will help to enhance the therapeutic benefit and to reduce the side effects (Cheng *et al*., 2022; Timin *et al*., 2022). The nanoparticles can be coupled with a targeting ligand that can specifically bind to receptors overexpressed on the membrane of cancer cells in order to actively convey the nanoparticles into tumor cells (Yu *et al*., 2010; Bazak *et al*., 2015; Lei *et al*., 2022). Proteins, folate, transferrin, hyaluronic acid, carbohydrates, antibodies, peptides, and aptamers are only a few examples of the unique ligands that can be employed in the NP structure to target various cancer locations and achieve the active strategy (Stella *et al*., 2000; Cardoso *et al*., 2012; Huang and Huang, 2018;

Jeong *et al*., 2018; Muhamad *et al*., 2018; Zhang *et al*., 2018; Liu *et al*., 2022).

Transferrin (Tf) is a glycoprotein that facilitates iron-uptake in cells. It binds to and consequently mediates the transport of iron (Fe) through blood plasma. Iron-loaded Tf first binds to the Tf receptor (TfR) and enters the cell through clathrin-mediated endocytosis (Mayle *et al*, 2012; Ogun and Adeyinka, 2022). Several studies have shown that cancer cells often overexpress the transferrin receptor (TfR) compared to normal cells. This is because malignant cancer cells require more iron for their growth and rapid proliferation (Nogueira-Librelotto *et al*., 2017; Daniels *et al*., 2012; Shen *et al*., 2018). *Annonaceous acetogenins* from *Annona muricata* Lin all have similar chemical structures and often consist of long aliphatic 35–37 carbon chains, a lactone ring, and no more than three tetrahydrofuran rings (Liaw *et al*., 2010; Moghadamtousi *et al*., 2015). Annonaceous acetogenins, or ACGs, have been shown to have powerful, selective anticancer properties by preventing cancer cells from migrating and invading by disrupting the mitochondrial membrane, which triggers death (Moghadamtousi *et al*., 2014; Pieme *et al*., 2014). Researchers have examined the anticancer activity of *Annonaceous acetogenins* in a variety of cancer cells, including leukemia, breast cancer, and lung cancer, and found that the IC_{50} was less than 20 g/mL (Moghadamtousi *et al*., 2014; Pieme *et al*., 2014; Moghadamtousi *et al*., 2015; Gavamukulya *et al*., 2017; Coria-Téllez *et al*., 2018). Although this category of biomolecules shows a promising action against cancer cells, they also exhibited non-specific toxicity toward normal tissue, leading to undesirable consequences like neurotoxicity and nephrotoxicity (Abdul Wahab *et al*., 2018). However, more research is needed to fully understand their selectivity and potential as an anti-cancer treatment. The use of delivery methods based on nanotechnology can solve problems associated with the high toxicity of chemical methods of synthesizing nanopar-ticles. The green synthesis of gold nanoparticles using *Annona muricata* extract and the increased erythrocyte osmotic fragility that was described in our earlier investigations is one such technique (Avan *et al*., 2018).

A low conductance state of the permeability transition pore complex (PTPC), which is primarily regulated by mitochondrial solute carriers, may help with the exchange of small metabolites between the cytosol and mitochondrial matrix under physiological conditions. Mitochondria also have a strong mitochondrial transmembrane potential. PTPC would consist of cyclophilin D (CyPD) in the mitochondrial matrix, voltage-dependent anion channels in the outer membrane, and adenine nucleotide translocase in the inner membrane. PTP inhibition, blocking the increase in mitochondrial calcium or reactive oxygen species that activate PTP are all possible methods to decrease PTP opening (Bauer *et al*., 2020; Bonora *et al*., 2022). Acetogenin nano-formulations have been synthesized using poly(caprolactone)–co-poly (ethylene glycol) (PCL-PEG) (Hong *et al*., 2016) and DSPE-PEG-FA and soybean lecithin (SPC) as carriers and stabilizers, respectively (Li *et al.,* 2018). Also, mPEG2000–PCL2000 amphiphilic block polymer has been used (Hong *et al*., 2016). The efficacy of PEGylated Liposomes has been studied where non-cytotoxic Stearyl triphenylphosphonium (STPP)-modified liposomes conjugated with polyethylene glycol and phosphatidylethanolamine (PEG-PE) to ensure a targeted delivery to the mitochondria (Biswas *et al*., 2012). This polymer modification possibility can broaden the use of PEG in the delivery of bioactive molecules from plants for the treatment of cancer. To the best of our knowledge, there is currently no PEG-based delivery nano-system conjugated with transferrin that has potential for the targeted distribution of *Annonaceous acetogenin* that has been reported.

MATERIALS AND METHODS

Materials used

Annonaceous acetogenin (Annomricin E) was generously provided by the medicinal plant research institute, Lagos, Nigeria, human holo-transferrin, dioxane, N-hydroxysuccinimide (NHS), and 1-ethyl-3-(3-dimethylaminopropyl) carbodiimine (EDC) are products of Sigma-Aldrich (St. Louis, MO, USA), N-Succinimidyl-S-acetylthioacetate (SATA) (Pierce Biotechnology) in dimethylformamide (DMF), N, N-disuccinimidyl carbonate (DSC) (Pierce Biotechnology), Polyethylene gycol (HO-PEG-NH2; MW: 5,000) (Laysan Bio), 5 nm standard gold nanoparticle (Cytodiagnostic, Canada). Dulbecco's Modified Eagle's Medium (DMEM), fetal bovine serum (FBS), phosphate buffered saline (PBS), L-glutamine solution (200 mM), trypsin-EDTA solution (170,000 U/L trypsin and 0.2 g/L EDTA), and penicillin-streptomycin solution (10,000 U/mL penicillin and 10 mg/mL streptomycin) were from Lonza (Verviers, Belgium).

Preparation of peg-GNPs, peg-ACGs and T_f-PEG-G-ACGs

For preparation of peg-GNPs, peg-ACGs and T_f-peg-G-ACGs, the methods of Krishna *et al*. (2006) and Choi *et al*. (2010) methods were adopted with modification. Briefly, PEG-SH was mixed with an aqueous suspension of 100-nm unmodified AuNPs to initiates the assembly of PEG-AuNPs, which was followed by the addition of a mixture of Transferrin protein solution combined with pre-weighted *Annonaceous acetogenin* (ACGs) in 10 mg EDC at 25°C for 2 h under probe sonication.

Physiochemical characterization the nano-formulations

By following already established protocols, the mean

hydrodynamic diameter and the polydispersity index (PDI) were analyzed by dynamic light scattering (DLS) in a Malvern Zetasizer ZS (Malvern Instruments, Malvern, UK). The Tf-peg-ACGs nanoparticles were characterized for the rate of protein conjugation using a commercial kit (BioRad® assay, CA, USA) based on the Bradford dye-binding procedure following the manufacturer protocol (Bradford, 1976). Each measurement was performed at least three times at 595 nm using a double-beam UV-Vis spectrophotometer (UV-1800, Shimadzu, Japan). The morphology of the NPs was analyzed by transmission electron microcopy (TEM) (1200EX, JEOL, USA).

Drug loading and encapsulation efficiency

The drug loading (DL) and encapsulation efficiency (EE%) were quantified using a high-performance liquid chromatography (HPLC) method, which was validated following a previously published procedure (Sun *et al*., 2001) with some modifications. Briefly, the column was kept at a constant temperature of 45.0 ± 0.2°C and the flow rate was set at 1.0 mL/min. The mobile phase was composed of methanol and water in a 90:10 ratio. The elution was monitored for 8 minutes and the compounds ACGs was detected at a wavelength of 220 nm. Squamostatin-B, squamocin and annonin-VI were used as standard substances. Samples were kept at 4.0 ± 0.5°C during the analysis.

Experimental animals

Male Wistar rats were allowed to acclimatize in the Preclinical Animal Holding Facility of the Department of Biochemistry, University of Benin for two weeks. They were kept in standard and well-ventilated cages.

Isolation of rat liver mitochondria

The isolation was carried out as described by Johnson and Lardy (1967) and modified by Olorunsogo *et al*. (1979) which was reported by Lapidus and Sokolove (1993).

Mitochondrial protein determination

Mitochondrial protein was determined with bovine serum albumin as standard (Lowry *et al*., 1951).

Mitochondria swelling assay

Mitochondrial membrane permeability transition as well as mitochondria swelling were determined according to already established method (Zoratti and Szabò, 1995). Swelling was measured as a decrease in absorbance within the time space of 12 minutes. The temperature was maintained at 37°C and the swelling rate quantified at A540/min/mg (Oyedeji *et al*., 2017).

Statistical analysis of data

Statistical analyses were performed using Origin Pro 2020 (Origin Lab Corporation, Northampton, MA, USA). Comparison between groups was performed using the Turkey's test. Comparison of the variables was made using the ANOVA and the results were considered statistically significant at $p < 0.05$, 0.01, and 0.001.

Ethical approval

The work was approved by the Faculty of Life Sciences Ethical Review Committee (UB10523) and conducted with the Guide for the Care and Use of Laboratory Animals (National Research Council, 2011).

RESULTS

Figure 1 shows the schematic representation of the functionalized nanoparticles. Conjugation was successful after probe sonication at a pH of 7.4. Figure 2 shows the Uv-vis spectrum of the non-functionalized Peg-AGCs and functionalized Tf-Peg-G-ACGs. A distinctive optical property of gold nanoparticles is known as localized surface plasmon resonance (LSPR), which is the collective oscillation of gold nanoparticle electrons in their conduction band in resonance with a particular wavelength of received light. UV-Vis spectroscopy can be used to measure the strong absorbance band that emerges from the LSPR of gold nanoparticles in the visible spectrum (500–600 nm). The conjugation of transferrin and pegylation did not change this behavior. Figure 3 shows the dynamic Light Scattering (DLS) of the non-functionalized Peg-AGCs and functionalized T_f-Peg-G-ACGs. The particles followed a normal distribution suggestive of their monodispersity. Plate 1 reveals a reduced size of the functionalized nanoparticles with no evidence of agglomeration.

Table 1 presented the physiochemical characteristics of ACGs-loaded pegylated nanoparticles, the particle sizes are not significance different with or without conjugation. The polydispersity index is satisfactorily low, the zeta potential fall within the recommended region while the drug loading and entrapment efficiency were significantly different for the functionalized and non-functionalized nanoparticles. Figure 4 shows the *in vitro* cumulative release profiles of ACGs at physiological conditions. The release profile was slow during the 24 h period before a burst tantamount to a non-Fickian diffusion. Overall, the

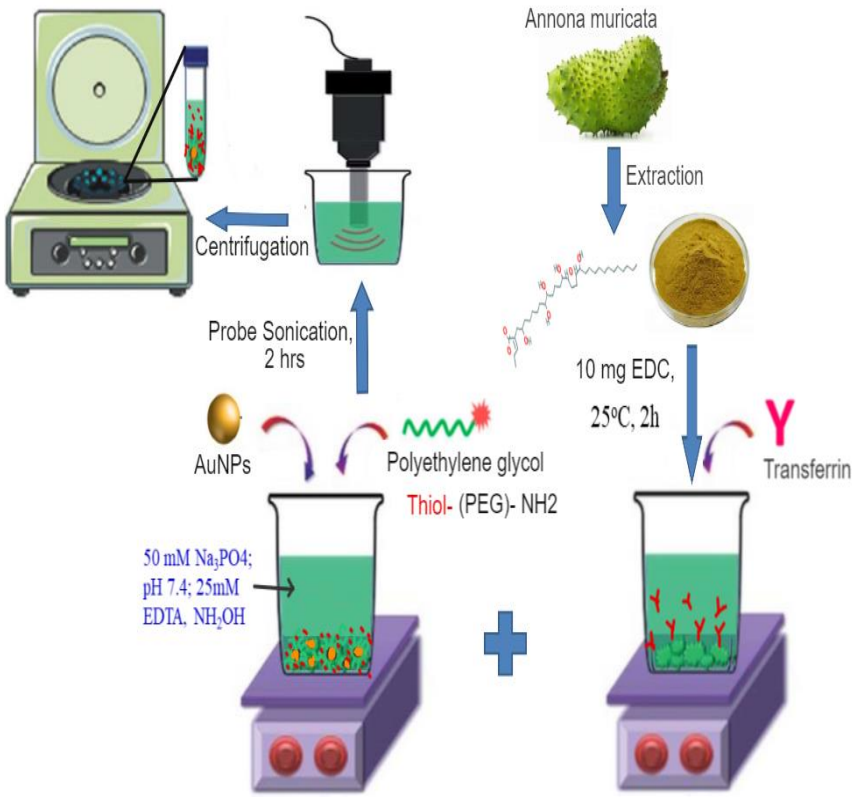

Figure 1. Schematic representation of the synthesized process of the functionalized nanoparticles.

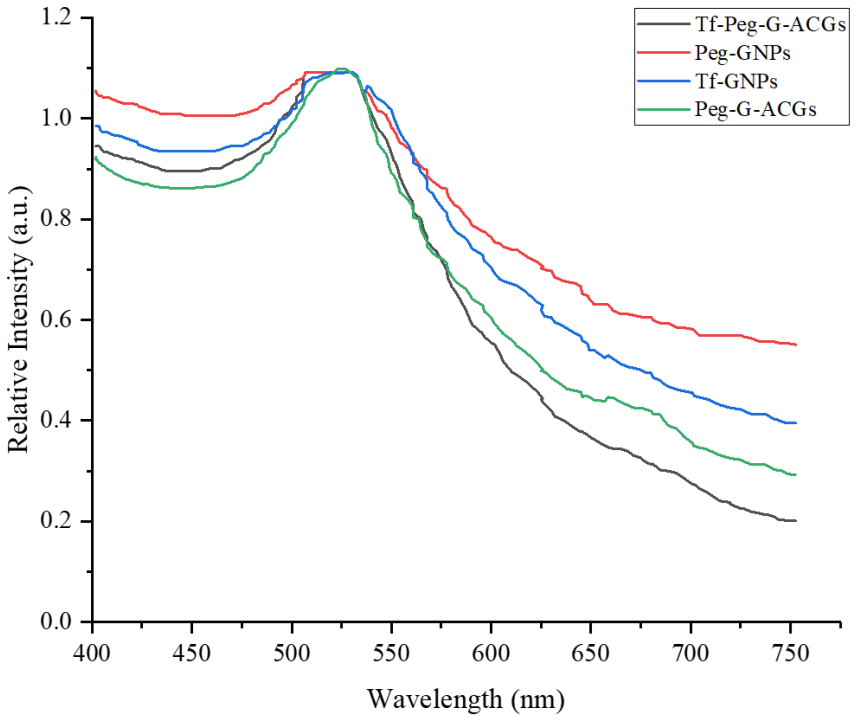

Figure 2. UV spectrum of functionalized and non-functionalized nanoparticles.

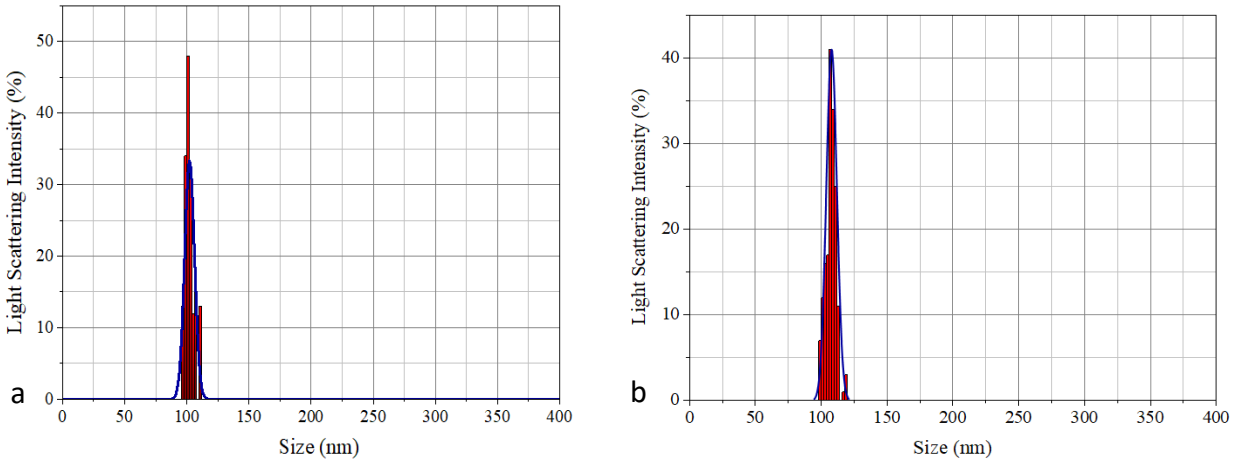

Figure 3. Dynamic Light Scattering (DLS) of (a) Peg-AGCs and (b) T_f-Peg-G-ACGs.

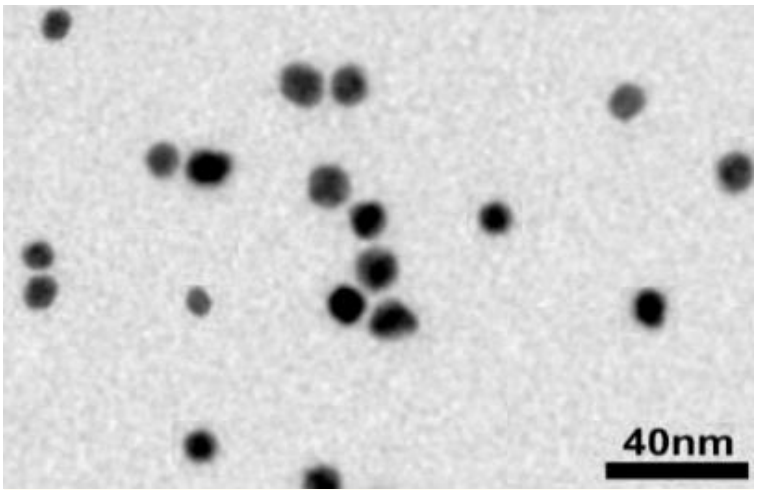

Plate 1. TEM micrograph of Tf-PEG-ACGs.

Table 1. Characteristics of acetogenins (ACGs) loaded pegylated Nanoparticles.

Parameters	Diameter (nm)	PDI	Zeta-potential (mV)	Drug Loading (%)	Drug encapsulation (%)
Tf-GNPs	110 ± 2	0.50 ± 0.010	- 36 ± 2.3	-	-
Peg-ACGs	130 ± 3	0.37 ± 0.020	- 14 ± 1.5	53	90
Tf-Peg-G-ACGs	170 ± 1	0.25± 0.010	- 10 ± 3.3	36	87

functionalized nanoparticles showed a plausible release up to about 85% for the 96 h period. Figure 5 illustrates that over a 12 minutes period, there was no change in the absorbance. However, there was a considerable amplitude mPT pore opening upon the injection of exogenous calcium (Triggering Agent), which was greatly inhibited by spermine, a common inhibitor. This demonstrates that the mitochondria employed in this study were healthy mitochondria.

In the absence of calcium (Figure 6a), Tf-peg-G-ACGs caused a concentration-dependent induction of mPT pore opening by 13, 11.3, 8.7, and 2.7 folds, at concentrations 10, 20, 50 and 100 µg/mL, respectively, when compared with the control. The swelling process was characterized by the time needed to reach the half-maximal light scattering signal (T1/2) (Figure 6b). The result revealed a significant difference between treatments and control. Furthermore, in the presence of calcium (Figure 7a), mPT

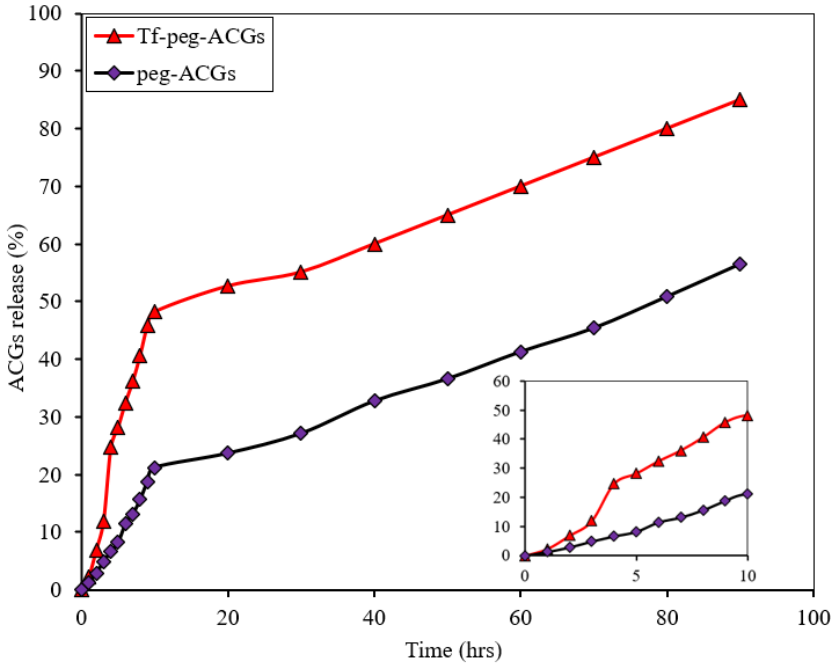

Figure 4. The in vitro cumulative release profiles of ACGs at 37°C in pH 7.4 PBS. All data represent the mean ± SD (n=3). ACGs. annonaceous acetogenins.

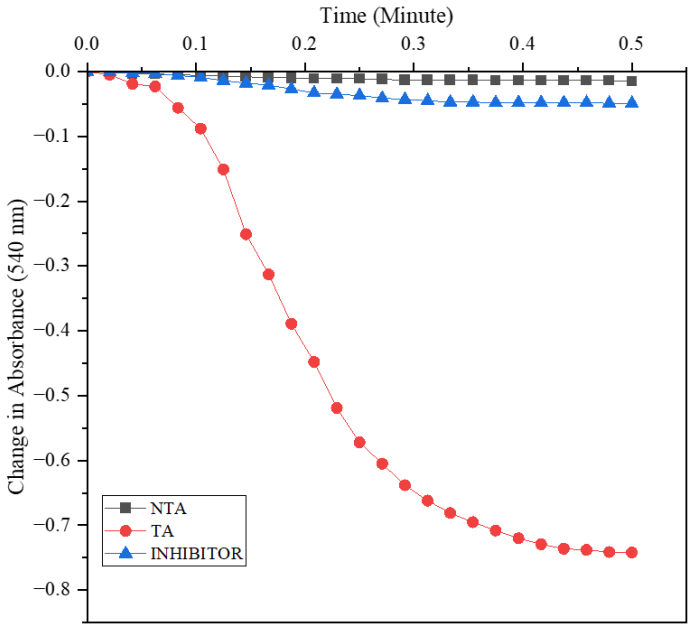

Figure 5. In vitro Ca^{2+} - induced mitochondrial swelling and inhibition of the opening by spermine. NTA: No triggering agent, TA: Triggering agent, INHIBITOR: Spermine.

pore opening was intensified by Tf-peg-G-ACGs by 22, 19.7, 15 and 8.3 folds at concentrations 10, 20, 50 and 100 µg/mL, respectively, when compared with the control. The results of half-time maximum light scattering signal (Figure 7b) revealed a significant difference between all treatments and control.

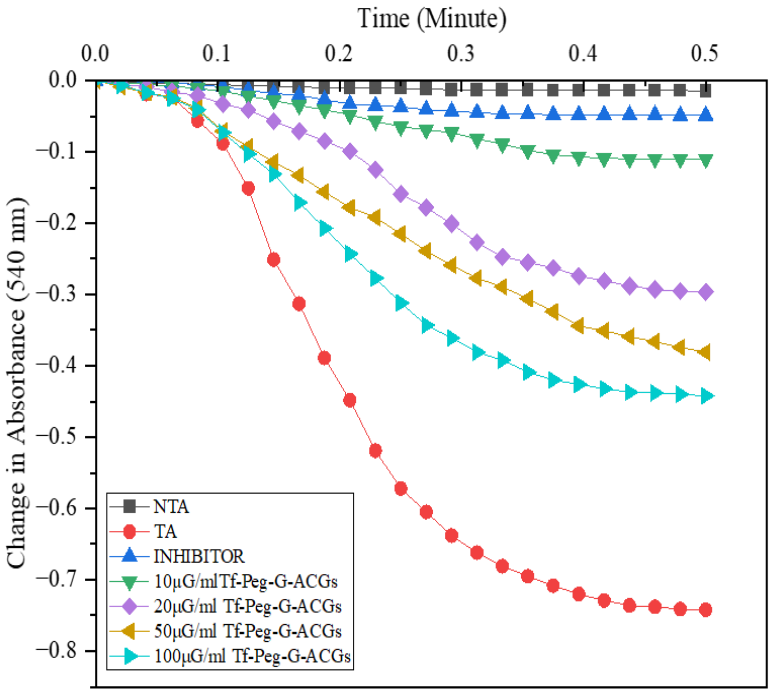

Figure 6a. In vitro induction of rat liver mitochondrial membrane permeability transition pore opening by varying concentrations of Tf-peg-G-ACGs in the absence of Calcium. NTA: No triggering agent, TA: Triggering agent, INHIBITOR: Spermine.

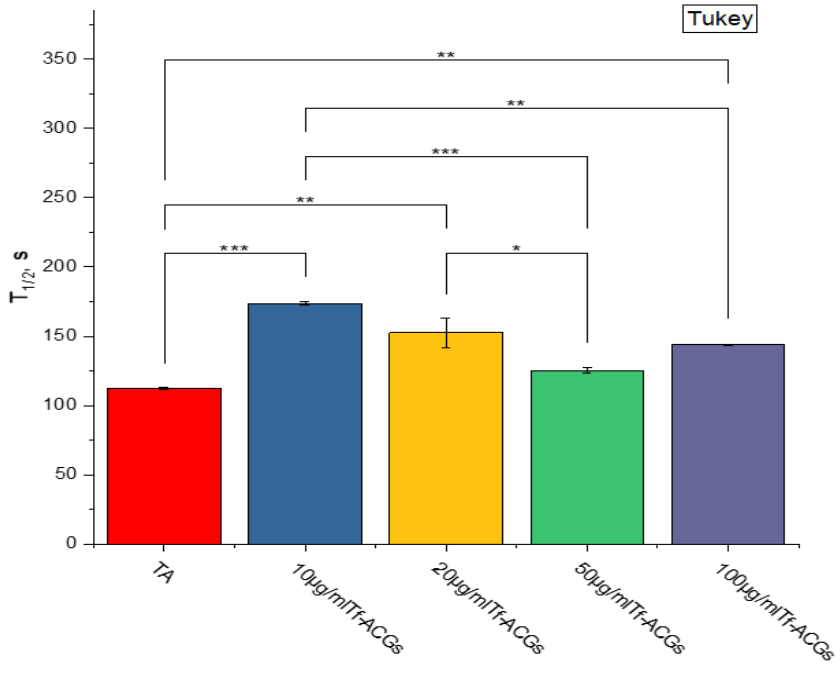

* p<=0.05 ** p<=0.01 *** p<=0.001

Figure 6b. half-maximal light scattering signal (T1/2). The values shown are the means ±SD from three independent experiments. TA: Triggering agent.

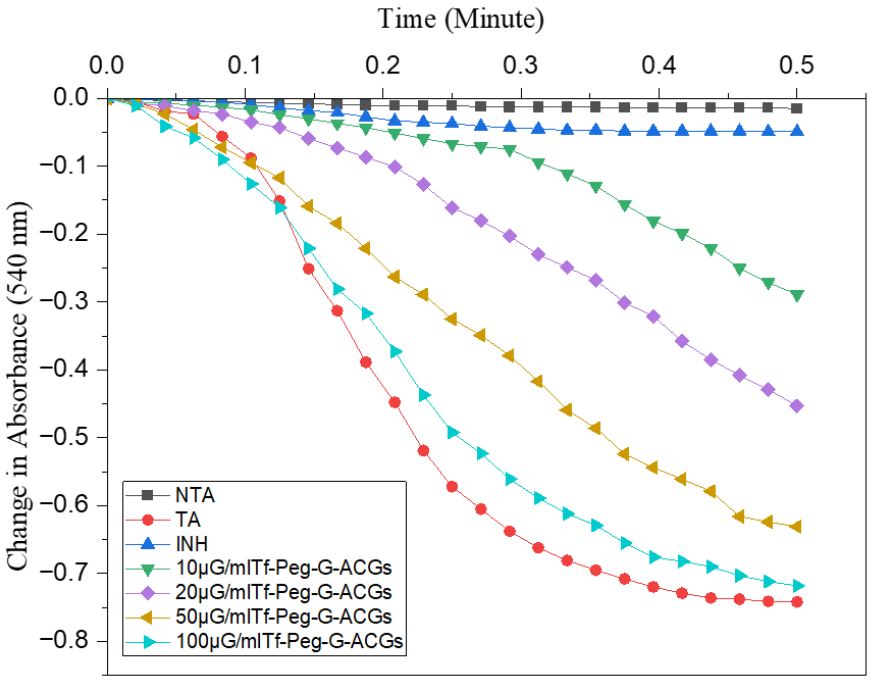

Figure 7a. *In vitro* induction of rat liver mitochondrial membrane permeability transition pore opening by varying concentrations of Tf-peg-G-ACGs in the presence of Calcium. NTA: No triggering agent, TA: Triggering agent, INHIBITOR: Spermine.

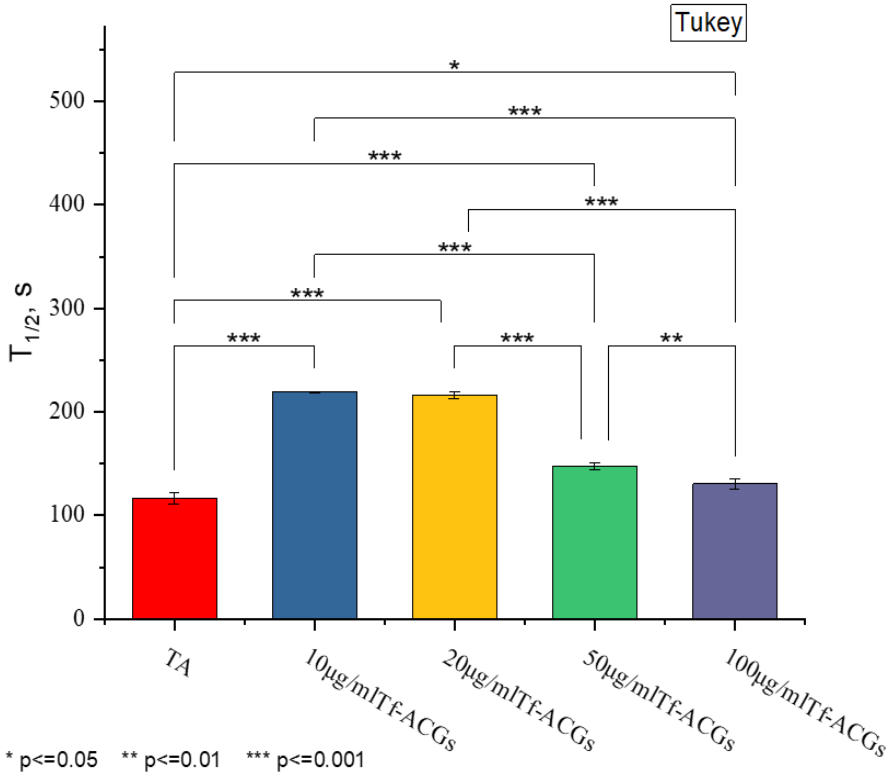

Figure 7b. half-maximal light scattering signal (T1/2). The values shown are the means ±SD from three independent experiments. TA: Triggering agent.

DISCUSSION

A lot of effort has been devoted to achieving active targeting for cancer therapy in order to reach the right cells. Notably, active targeting nanoparticles have shown improved therapeutic performances in different tumor models as compared to their passive targeting counterparts. Few issues arise with traditional chemotherapy, such as ineffective delivery of treatment regimens to the tumor solely and at the proper concentration (Cryer and Thorley, 2019).

The complete strategy to develop a receptor-targeted drug delivery system by probe sonication of acetogenins-loaded transferrin conjugated nanoparticles was shown in Figure 1. The ability of peg-G-NPs to imitate the flow patterns of actual therapeutic nanoparticles makes them useful as model agents for optimizing drug delivery systems (Chenthamara *et al*., 2019). T_f-GNPs was employed as a transferrin receptor targeting ligand to deliver the acetogenins to transferrin receptor site (Nicolas *et al*., 2013). The blank Tf-GNPs had a diameter of 110 ± 2 nm with PDI of 0.50 ± 0.010 and ZP of − 36 ± 2.3 mV and the peg-ACGs had a diameter of 130 ± 3 nm with PDI of 0.37 ± 0.020 and ZP of − - 14 ± 1.5 mV (Table 1). After entrapment of ACGs, the particle size increased to 170 ± 1 nm and while the PDI decreased to 0.25 ± 0.010. However, the ZP values became less negative (- 10 ± 3.3 Mv) due to the shielding effect on the charge of Tf caused by the ACGs nearby to the surface of the nanoparticles.
The DLS characterization revealed narrowly distributed particles with an average size of about 100 nm for peg-ACGs. The conjugation of transferrin however, cause a small increase in the nanometric size of the Tf-peg-ACGs nanoparticles, but with no significant difference. The results in this study are in-line with several reports in which transferrin was used as a targeting moiety (Nicolas *et al*., 2013; Tavano *et al*., 2014; Scheeren *et al*., 2020). The drug loading and encapsulation studies revealed that percentage drug loading capacity of peg-ACGs (53%) was higher than that of Tf-peg-ACGs (36%) possibly due to competition between the Tf- and ACGs whereas the percentage entrapment efficiency was not significantly different with peg-ACGs with 90% while Tf-peg-ACGs with 87%. The pH of the tumor region (pH_e) ranges between 6.5 to 7.2 and of the lyso-endosomal compartments that ranges from 5.0 to 6.5 are generally lower than those of normal tissues, which have pH values in the physiological range of 7.35 to 7.45. This makes the pH a more universal approach for tumor targeting, through pH-sensitive delivery systems (Lee *et al*., 2007; Tian and Bae, 2012). To this end, the pH of the aqueous phase was set to 7.4 to regulate the polarity of the ACGs, boost its lipophilicity, and increase the effectiveness of entrapment.

The cumulative dissolution profiles (Figure 3) reveal that the Tf-peg-ACGs nanoparticles release the acetogenins content better than the peg-ACGs at pH 5.5 an indication of a high payload of ACGs to be delivered to tumor which may lead to a possible enhancement in the efficacy. The observation of the early events revealed no notable drug burst release behavior in the first 3 h with only 11.87% of the acetogenins that were encapsulated released. However, there was a burst before 10 h period resulting in the accumulated release of up to 44.38% of acetogenins. This release mechanism led to the cumulative ACGs release of 50.16% in 24 h. Comparatively, peg-ACGs nanoparticles demonstrated a slower early release, with 3 h release at 5.2% and 10 h release up to 10%. The cumulated ACGs release stayed at 25.9% at 24 h. Analysis of the release mechanism of the Tf-peg-ACGs nanoparticles showed non-Fickian diffusion ($n > 0.43$) and a first order kinetics. This is opposed to the formulation of Scheeren *et al*. (2020), that observed a Fickian diffusion, in the release of doxorubicin from pH responsive Transferrin-conjugated doxorubicin-loaded PLGA nanoparticles T_f-DOX-PLGA-NPs PBS pH 7.4, 6.6, and 5.4, with $n = 0.28$, 0.31, and 0.35, respectively.

Many incoming stress signals are processed by the mitochondrion, and abnormalities in the mitochondria frequently appear before any clear morphological evidence of apoptosis. It has long been recognized that the mPT pore can be used as a pharmacological target when developing medications to treat various cancers and tumors.

After determining the intactness of the mitochondrion to ascertain its integrity, the results on the effect of Tf-peg-G-ACGs on mPT pore showed a concentration-dependent induction of mPT pore opening in the absence of calcium when compared with the NTA. This suggests that Tf-peg-G-ACGs release the loaded acetognins into the mitochondria to facilitated its already well-established cytotoxic effect leading to induced mPT pore opening. When Ca^{2+} at the threshold concentration was added to the mitochondrial suspension incubated in the standard, light scattering—a hallmark of mitochondrial enlargement decreased. Further evidence that Tf-peg-G-ACGs did not compromise the integrity of mitochondria comes from the fact that the common inhibitor spermine reversed the mPT pore opening that was caused by Tf-peg-G-ACGs. Additionally, the pore opening was worsened in the presence of calcium as the $T_{1/2}$ was shortened compared to control, indicating a greater sensitivity of mitochondria to Ca^{2+} and mPTP initiation.

Interestingly, while the modulation of the mitochondrial membrane by Tf-peg-G-ACGs does not indicate a cell's definitive commitment to death, it is a significant step toward its application in the treatment of cancer, particularly those with high transferrin receptors such as colorectal cancer.

Conclusion

This study successfully developed targeting nanocarrier for ACGs delivery, comprising of PEG, gold nanoparticles

and transferrin protein. Characterization of the formulation showed physicochemical properties expected of a drug delivery system (DDS). The main advantages of the Tf-peg-G-ACGs is their small size and ability to deliver highly hydrophobic bioactive molecules as acetogenin in this instance compared to whole molecule or non-functionalized pegylated molecules. It suffices to say that the conjugation of acetogenin-loaded nanoparticles with transferrin is a feasible way of delivering bioactive molecules directly to cancer cells as revealed by the aggravated mitochondrial membrane pore opening

CONFLICTS OF INTEREST

The authors declare that they have no conflicts of interest.

REFERENCES

Abdul Wahab, S. M., Jantan, I., Haque, M. A., & Arshad, L. (2018). Exploring the Leaves of Annona muricata L. as a Source of Potential Anti-inflammatory and Anticancer Agents. *Frontiers in pharmacology*, 9, 661.

Avan, E. D., Quadry, R. O., Ikenna-Ossai, C. N., & Okolie, N. P. (2018). Effects of Annona muricata Biofunctionalized Gold Nanoparticles on Erythrocyte Osmotic Fragility and Hematological Profile in Rat Model. *Covenant Journal of Physical and Life Sciences*, 2(1), 33-45

Bauer, T. M., & Murphy, E. (2020). Role of Mitochondrial calcium and the permeability transition pore in regulating cell death. *Circulation Research*, 126(2), 280-293.

Bazak, R., Houri, M., El Achy, S., Kamel, S., & Refaat, T. (2015). Cancer active targeting by nanoparticles: a comprehensive review of literature. *Journal of Cancer Research and Clinical Oncology, 1*41(5), 769-784.

Biswas, S., Dodwadkar, N. S., Deshpande, P. P., & Torchilin, V. P. (2012). Liposomes loaded with paclitaxel and modified with novel triphenylphosphonium-PEG-PE conjugate possess low toxicity, target mitochondria and demonstrate enhanced antitumor effects *in vitro* and *in vivo*. *Journal of Controlled Release: Official Journal of the Controlled Release Society*, 159(3), 393-402.

Bonora, M., Giorgi, C., & Pinton, P. (2022). Molecular mechanisms and consequences of mitochondrial permeability transition. Nature reviews. Molecular cell biology, *23*(4), 266-285.

Bradford, M. M. (1976). A rapid and sensitive method for the quantitation of microgram quantities of protein utilizing the principle of protein-dye binding. Analytical biochemistry, 72, 248-254.

Cardoso, M. M., Peça, I. N., & Roque, A. C. (2012). Antibody-conjugated nanoparticles for therapeutic applications. *Current Medicinal Chemistry*, 19(19), 3103-3127.

Cheng, W. J., Chuang, K. H., Lo, Y. J., Chen, M., Chen, Y. J., Roffler, S. R., Ho, H. O., Lin, S. Y., & Sheu, M. T. (2022). Bispecific T-cell engagers non-covalently decorated drug-loaded PEGylated nanocarriers for cancer immunochemo-therapy. *Journal of Controlled Release: Official Journal of the Controlled Release Society*, 344, 235-248.

Chenthamara, D., Subramaniam, S., Ramakrishnan, S. G., Krishnaswamy, S., Essa, M. M., Lin, F.-H., & Qoronfleh, M. W. (2019). Therapeutic efficacy of nanoparticles and routes of administration. Biomaterials Research, *23*(1),1-29.

Choi, C. H., Alabi, C. A., Webster, P., & Davis, M. E. (2010). Mechanism of active targeting in solid tumors with transferrin-containing gold nanoparticles. *Proceedings of the National Academy of Sciences of the United States of America*, *107*(3), 1235-1240.

Coria-Téllez, A., Montalvo-Gonzalez, E., Yahia, E., & Obledo--Vázquez, E. (2018). *Annona muricata*: a comprehensive review on its traditional medicinal uses, phytochemicals, pharmacological activities, mechanisms of action and toxicity. *Arabian Journal of Chemistry*, *11*(5), 662-691.

Cryer, A. M., & Thorley, A. J. (2019). Nanotechnology in the diagnosis and treatment of lung cancer. Pharmacology & therapeutics, *198*, 189-205.

Daniels, T. R., Bernabeu, E., Rodríguez, J. A., Patel, S., Kozman, M., Chiappetta, D. A., Holler, E., Ljubimova, J. Y., Helguera, G., & Penichet, M. L. (2012). The transferrin receptor and the targeted delivery of therapeutic agents against cancer. Biochimica et biophysica acta, *1820*(3), 291-317.

Dutta, B., Barick, K. C., & Hassan, P. A. (2021). Recent advances in active targeting of nanomaterials for anticancer drug delivery. Advances in Colloid and Interface Science, *296*, 102509.

Fang, R. H., Gao, W., & Zhang, L. (2022). Targeting drugs to tumours using cell membrane-coated nanoparticles. *Nature Reviews Clinical Oncology*, 20(1), 33-48.

Gavamukulya, Y., Wamunyokoli, F., & El-Shemy, H. A. (2017). Annona muricata: Is the natural therapy to most disease conditions including cancer growing in our backyard? A systematic review of its research history and future prospects. *Asian Pacific Journal of Tropical Medicine*, *10*(9), 835-848.

Gavas, S., Quazi, S., & Karpiński, T. M. (2021). Nanoparticles for cancer therapy: current progress and challenges. *Nanoscale Research Letters*, 16, Article Number 173.

Hong, J., Li, Y., Li, Y., Xiao, Y., Kuang, H., & Wang, X. (2016). *Annonaceous acetogenins* nanosuspensions stabilized by PCL-PEG block polymer: significantly improved antitumor efficacy. *International Journal of Nanomedicine*, *11*, 3239-3253.

Huang, G., & Huang, H. (2018). Application of hyaluronic acid as carriers in drug delivery. *Drug Delivery*, *25*(1), 766–772.

Jeong, W. J., Bu, J., Kubiatowicz, L. J., Chen, S. S., Kim, Y., & Hong, S. (2018). Peptide-nanoparticle conjugates: a next generation of diagnostic and therapeutic platforms? *Nano Convergence*, 5, Article number 38.

Johnson, D., & Lardy, H. (1967). [15] Isolation of liver or kidney mitochondria. In *Methods in Enzymology* (Vol. 10, pp. 94-96). Academic Press.

Krishna, A. D. S., Mandraju, R. K., Kishore, G., & Kondapi, A. K. (2009). An efficient targeted drug delivery through apotransferrin loaded nanoparticles. *PloS one*, *4*(10), e7240.

Lapidus, R. G., & Sokolove, P. M. (1993). Spermine inhibition of the permeability transition of isolated rat liver mitochondria: an investigation of mechanism. *Archives of Biochemistry and Biophysics*, *306*(1), 246-253.

Lee, E. S., Oh, K. T., Kim, D., Youn, Y. S., & Bae, Y. H. (2007). Tumor pH-responsive flower-like micelles of poly(L-lactic acid)-b-poly(ethylene glycol)-b-poly(L-histidine). *Journal of Controlled Release: Official Journal of the Controlled Release Society*, 123(1), 19-26.

Lei, W., Yang, C., Wu, Y., Ru, G., He, X., Tong, X., & Wang, S. (2022). Nanocarriers surface engineered with cell membranes for cancer targeted chemotherapy. *Journal of Nanobiotechno-*

logy, *20*(1),1-21.
Li, H., Li, Y., Ao, H., Bi, D., Han, M., Guo, Y., & Wang, X. (2018). Folate-targeting *Annonaceous acetogenins* nanosuspensions: significantly enhanced antitumor efficacy in HeLa tumor-bearing mice. *Drug Delivery*, 25(1), 880-887.
Liaw, C. C., Wu, T. Y., Chang, F. R., & Wu, Y. C. (2010). Historic perspectives on *Annonaceous acetogenins* from the chemical bench to preclinical trials. *Planta Medica*, *76*(13), 1390-1404.
Liu, M., Wang, L., Lo, Y., Shiu, S. C. C., Kinghorn, A. B., & Tanner, J. A. (2022). Aptamer-enabled nanomaterials for therapeutics, drug targeting and imaging. *Cells*, *11*, Article number 159.
Lowry, O. H., Rosebrough, N. J., Farr, A. L., & Randall, R. J. (1951). Protein measurement with the Folin phenol reagent. *The Journal of Biological Chemistry*, *193*(1), 265-275.
Mayle, K. M., Le, A. M., & Kamei, D. T. (2012). The intracellular trafficking pathway of transferrin. *Biochimica et Biophysica Acta*, 1820(3), 264-281.
Moghadamtousi, S. Z., Fadaeinasab, M., Nikzad, S., Mohan, G., Ali, H. M., & Kadir, H. A. (2015). *Annona muricata* (Annonaceae): A review of its traditional uses, isolated acetogenins and biological activities. *International Journal of Molecular Sciences*, *16*(7), 15625-15658.
Moghadamtousi, S. Z., Karimian, H., Rouhollahi, E., Paydar, M., Fadaeinasab, M., & Abdul Kadir, H. (2014). Annona muricata leaves induce G_1 cell cycle arrest and apoptosis through mitochondria-mediated pathway in human HCT-116 and HT-29 colon cancer cells. *Journal of Ethnopharmacology*, 156, 277-289.
Muhamad, N., Plengsuriyakarn, T., & Na-Bangchang, K. (2018). Application of active targeting nanoparticle delivery system for chemotherapeutic drugs and traditional/herbal medicines in cancer therapy: a systematic review. *International Journal of Nanomedicine*, *13*, 3921-3935.
National Research Council (2011). Committee for the Update of the Guide for the Care and Use of Laboratory Animals. Guide for the Care and Use of Laboratory Animals. 8th edition. Washington (DC): National Academies Press (US). Retrieved from https://www.ncbi.nlm.nih.gov/books/NBK54050/
Nicolas, J., Mura, S., Brambilla, D., Mackiewicz, N., & Couvreur, P. (2013). Design, functionalization strategies and biomedical applications of targeted biodegradable/biocompatible polymer-based nanocarriers for drug delivery. *Chemical Society Reviews*, 42(3), 1147-1235.
Nogueira-Librelotto, D. R., Codevilla, C. F., Farooqi, A., & Rolim, C. M. (2017). Transferrin-conjugated nanocarriers as active-targeted drug delivery platforms for cancer therapy. *Current Pharmaceutical Design*, 23(3), 454-466.
Ogun, A. S., & Adeyinka, A. (2022). Biochemistry, transferrin. In *StatPearls [Internet]*. StatPearls Publishing. Retrieved January 2023 from https://www.ncbi.nlm.nih.gov/books/NBK532928/
Olorunsogo, O., Bababunmi, E., & Bassir, O. (1979). The inhibitory effect of N-(phosphonomethyl) glycine in vivo on energy-dependent, phosphate-induced swelling of isolated rat liver mitochondria. *Toxicology Letters*, *4*(4), 303-306.
Oyedeji, T. A., Akintehinse, T., Avan, E. D., Soremekun, O. O., Solomon, O. E., & Olorunsogo, O. O. (2017). Extracts of *Adenopus breviflorus* induce opening of rat liver mitochondrial membrane permeability transition pore. *Biokemistri*, *29*(4), 140-145.
Pieme, C. A., Kumar, S. G., Dongmo, M. S., Moukette, B. M., Boyoum, F. F., Ngogang, J. Y., & Saxena, A. K. (2014). Antiproliferative activity and induction of apoptosis by Annona muricata (Annonaceae) extract on human cancer cells. *BMC complementary and Alternative Medicine*, *14,* Article number 516.
Scheeren, L. E., Nogueira-Librelotto, D. R., Macedo, L. B., de Vargas, J. M., Mitjans, M., Vinardell, M. P., & Rolim, C. M. (2020). Transferrin-conjugated doxorubicin-loaded PLGA nanoparticles with pH-responsive behavior: a synergistic approach for cancer therapy. *Journal of Nanoparticle Research*, *22*, Article number 72.
Shen, Y., Li, X., Dong, D., Zhang, B., Xue, Y., & Shang, P. (2018). Transferrin receptor 1 in cancer: a new sight for cancer therapy. *American Journal of Cancer Research*, *8*(6), 916-931.
Stella, B., Arpicco, S., Peracchia, M. T., Desmaële, D., Hoebeke, J., Renoir, M., D'Angelo, J., Cattel, L., & Couvreur, P. (2000). Design of folic acid-conjugated nanoparticles for drug targeting. *Journal of Pharmaceutical Sciences*, 89(11), 1452-1464.
Sun, L., Yu, J. G., Li, D. Y., Li, J., Yang, X. D., & Yang, S. L. (2001). Determination of annonaceous acetogenins in Annonaceae plants by HPLC. *Yao xue xue bao= Acta Pharmaceutica Sinica*, *36*(9), 683-685.
Tavano, L., Aiello, R., Ioele, G., Picci, N., & Muzzalupo, R. (2014). Niosomes from glucuronic acid-based surfactant as new carriers for cancer therapy: preparation, characterization and biological properties. *Colloids and Surfaces B: Biointerfaces*, *118*, 7-13.
Tian, L., & Bae, Y. H. (2012). Cancer nanomedicines targeting tumor extracellular pH. *Colloids and Surfaces B: Biointerfaces*, *99*, 116-126.
Timin, A. S., Postovalova, A. S., Karpov, T. E., Antuganov, D., Bukreeva, A. S., Akhmetova, D. R., Rogova, A. S., Muslimov, A. R., Rodimova, S. A., Kuznetsova, D. S., & Zyuzin, M. V. (2022). Calcium carbonate carriers for combined chemo-and radionuclide therapy of metastatic lung cancer. *Journal of Controlled Release*, *344*, 1-11.
Yu, B., Tai, H. C., Xue, W., Lee, L. J., & Lee, R. J. (2010). Receptor-targeted nanocarriers for therapeutic delivery to cancer. *Molecular Membrane Biology*, 27(7), 286-298.
Zhang, X., Huang, G., & Huang, H. (2018). The glyconanoparticle as carrier for drug delivery. *Drug Delivery*, 25(1), 1840-1845.
Zoratti, M., & Szabò, I. (1995). The mitochondrial permeability transition. *Biochimica et Biophysica Acta*, 1241(2), 139-176.